

First-order paramagnetic-to-commensurate phase transition in Cr alloys

R. S. Fishman

Solid State Division, P.O. Box 2008, Oak Ridge National Lab, Oak Ridge, Tennessee 37831-6032

X. W. Jiang*

Physics Department, North Dakota State University, Fargo, North Dakota 58105-5566

S. H. Liu

Physics Department, University of California, San Diego, California 92093

(Received 31 October 1997)

The coexistence of spin- and charge-density waves in pure Cr and its dilute alloys continues to fascinate both experimentalists and theorists. Using a three-band model, we show that the charge-density wave (CDW) in incommensurate (I) Cr alloys is governed by the same Coulomb interaction that produces a first-order Néel transition in commensurate (C) alloys. Therefore, we predict that the first-order paramagnetic-to-commensurate transition observed in CrFe and CrSi alloys is preceded by the growth of a large CDW in the I phase of each alloy. We also provide a justification for the three-band model in the I phase and show that it reduces to the correct form in the C limit. [S0163-1829(98)01225-9]

I. INTRODUCTION

Like superconductivity, spin- and charge-density waves are collective phenomena that involve large numbers of particles in coherent momentum states. Depending on doping levels and temperature, the spin-density wave (SDW) that appears below the Néel temperature of Cr alloys may be either commensurate (C) or incommensurate (I) with its bcc lattice.¹ In addition to being one of the few bulk systems containing a SDW, Cr also supports a charge-density wave (CDW) with twice the wave vector and half the period of the SDW. In this paper, we show that the same Coulomb interaction that governs the amplitude of the CDW in the I phase also produces a first-order paramagnetic (P) to C transition. Therefore, we predict that the first-order PC transition observed¹ in CrFe and CrSi alloys is preceded by the growth of a large CDW in the I phase of each alloy.

This prediction is based on a model that uses the random-phase approximation (RPA) in conjunction with one-electron band and two hole bands. Although the three-band model² may be easily justified in the I phase, its physical significance in the C phase is less clear. As discussed below, several objections may be raised to the use of the three-band model in the C phase of Cr alloys. We show that in the C limit, the three-band model reduces to a two-band model with a shifted hole energy. When this energy shift is sufficiently large, the PC transition becomes first order. Remarkably, the shift of the hole band in the C phase is produced by the same Coulomb interaction that determines the size of the CDW in the I phase.

Only one other theoretical work has addressed the question of the first-order PC transition in some Cr alloys. Unlike the present workers, Nakanishi and Kasuya³ studied the magnetostrictive effect of a volume expansion produced by the Fe impurities. This effect is not related to the presence of a CDW in the I phase. The results of Nakanishi and Kasuya will be discussed in the final section of this paper.

The SDW instability⁴ in Cr alloys is produced by the nearly perfect nesting^{5,6} of its electron a and hole b Fermi surfaces. As sketched in Fig. 1, both the electron Fermi surface centered at Γ and the hole Fermi surface centered at the zone boundary H are roughly octahedral in shape. Because the electron Fermi surface is slightly smaller than the hole Fermi surface, there are two different nesting wave vectors \mathbf{Q}_{\pm} that translate four faces of one Fermi surface onto four faces of the other. The Γ and H points are separated by $\mathbf{G}/2$, where \mathbf{G} is a reciprocal lattice vector with magnitude $4\pi/a$. Hence, the nesting wave vectors \mathbf{Q}_{\pm} lie on either side of $\mathbf{G}/2$ and may be written as $\mathbf{Q}_{\pm} = (\mathbf{G}/2)(1 \pm \delta)$, where $\delta \approx 0.05$ is a measure of the size difference between the electron and hole Fermi surfaces. Aside from the nested a and b Fermi surfaces, the band structure of Cr also contains two other

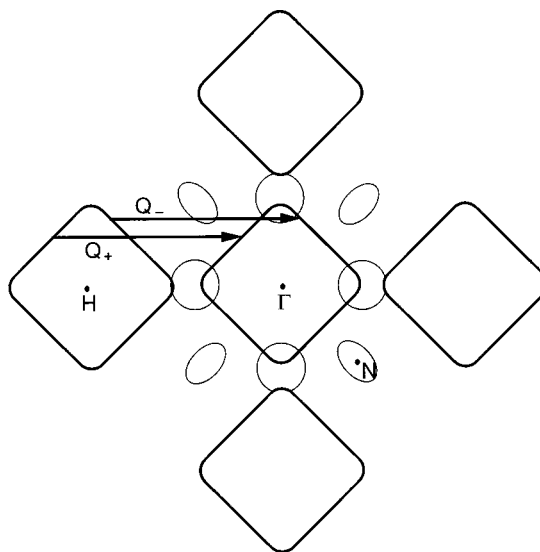


FIG. 1. The band structure of Cr alloys with Fermi surfaces a and b nested by the wave vectors \mathbf{Q}_{\pm} . Other Fermi surfaces constitute a reservoir band.

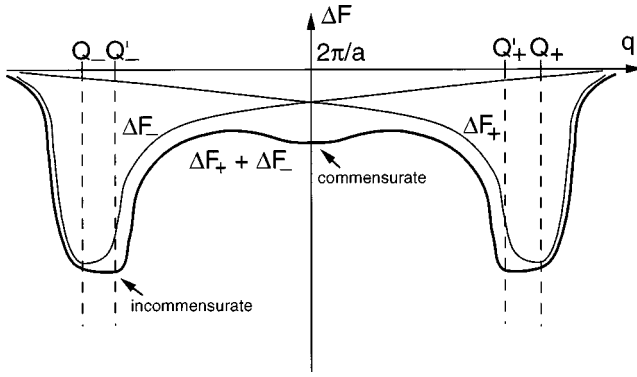


FIG. 2. A heuristic picture of the free-energy difference $\Delta F(q) = \Delta F_+(q) + \Delta F_-(q)$ between the paramagnetic and ordered states of Cr. The total free energy is plotted in the thick solid curve and the individual free energies $\Delta F_{\pm}(q)$ are plotted in the thin solid curves.

bands: one set is centered at the N points and the other lies midway between the Γ and H points.⁷ These non-nested Fermi surfaces play an ancillary role in the formation of the SDW and are often grouped together into an “electron reservoir.” The two-spin density of states of the nested and reservoir bands are given by ρ_{eh} and ρ_r .

While the condensate of a superconductor contains pairs of electrons with zero total momentum, the condensate of a spin-density wave contains pairs of electrons and holes with nonzero total momentum that may be related to the periodicity of the SDW. When incommensurate with the bcc lattice, the SDW of Cr actually contains two condensates of electron-hole pairs: one with pair momentum $\mathbf{Q}'_+ = (\mathbf{G}/2)(1 + \delta')$ and the other with pair momentum $\mathbf{Q}'_- = (\mathbf{G}/2)(1 - \delta')$. Because $0 \leq \delta' < \delta$, the ordering wave vectors \mathbf{Q}'_{\pm} of the SDW lie closer⁸ to $\mathbf{G}/2$ than the nesting wave vectors \mathbf{Q}_{\pm} . When $\delta' = 0$ and $\mathbf{Q}'_{\pm} = \mathbf{G}/2$, the SDW is commensurate with the lattice. Unlike \mathbf{Q}_{\pm} and δ , which are fixed by the band-structure topology, \mathbf{Q}'_{\pm} and δ' are solved by minimizing the nesting free energy ΔF and generally depend on temperature. In units of the lattice constant a , the period of the SDW is given by $1/\delta'$. For pure Cr just below its Néel temperature,¹ $\delta' \approx 0.037$ and $1/\delta' \approx 27$ so the SDW is very close to being commensurate.

The three sets of possible ordering wave vectors \mathbf{Q}'_{\pm} correspond to the three possible orientations of the nesting wave vectors along the (100), (010), or (001) directions. When pure Cr is cooled below the Néel temperature $T_N \approx 310$ K, six types of domains form.¹ In each domain, the spin polarization $\hat{\mathbf{m}}$ lies along one of two possible directions perpendicular to one of the three sets of wave vectors \mathbf{Q}'_{\pm} . The formalism developed in this paper describes one such domain, with a single polarization and one set of ordering wave vectors.

Heuristically, the difference between the nesting and ordering wave vectors can be easily understood. Imagine that the free-energy difference ΔF between the paramagnetic and ordered states can be separated into contributions from the nesting of the right and left faces of the electron and hole Fermi surfaces. The total free energy $\Delta F(q)$ (thick curve) and the individual contributions $\Delta F_{\pm}(q)$ (thin curves) with minima at \mathbf{Q}_{\pm} are sketched in Fig. 2. Since $\Delta F'_+(Q_-) < 0$

and $\Delta F'_-(Q_+) > 0$, the total free-energy difference $\Delta F(q)$ is not minimized at the nesting wave vectors \mathbf{Q}_{\pm} but rather at wave vectors \mathbf{Q}'_{\pm} that lie somewhat closer to $\mathbf{G}/2$. Although neither $\Delta F_+(q)$ nor $\Delta F_-(q)$ has a minimum at the commensurate wave vector $\mathbf{G}/2$, the total free energy contains such a minimum because $\Delta F'_+(q) = -\Delta F'_-(q)$ at $q = \mathbf{G}/2$. As the nesting wave vectors \mathbf{Q}_{\pm} are brought closer together by doping, the ordering wave vectors \mathbf{Q}'_{\pm} also approach $\mathbf{G}/2$. When δ is sufficiently small, the minimum in ΔF at $q = \mathbf{G}/2$ may become deeper than the minima near \mathbf{Q}_{\pm} . Then, the transition from the I to the C phase is first order. In the I phase, the location of the minima at \mathbf{Q}'_{\pm} depends on temperature through the shape of the free energies $\Delta F_{\pm}(q)$. Unfortunately, this appealing picture does not follow from a more precise derivation of the free energy ΔF within the three-band model: ΔF cannot be strictly divided into contributions ΔF_{\pm} from nesting on one side or the other of the two Fermi surfaces.

As first discussed by Young and Sokoloff,² who developed the three-band model, the CDW in Cr may be considered the second harmonic of the SDW. With wave vectors $2\mathbf{Q}'_{\pm}$, the CDW satellites lie on either side of the reciprocal lattice vector \mathbf{G} . Due to the periodicity of the Bloch wave functions $u(\mathbf{r})$, similar CDW satellites are found on either side of every other reciprocal lattice vector. This has been verified in a number of x-ray^{9,10} and neutron-scattering experiments,^{11,12} most recently by Hill and co-workers.¹³

Higher harmonics of the SDW have also been observed:¹ the third harmonics of the SDW lie at wave vectors $(\mathbf{G}/2)(1 \pm 3\delta')$ while the fourth harmonics of the SDW or, equivalently, the second harmonics of the CDW lie at wave vectors $\mathbf{G}(1 \pm 2\delta')$. Evidence¹ suggests that the amplitude of the n th harmonic is proportional to the amplitude of the fundamental to the n th power. Aside from the CDW, other harmonics are neglected by the three-band model.

Within the three-band model, the hole band is shifted by wave vectors \mathbf{Q}'_{\pm} while the electron band is kept fixed as shown in Fig. 3(a). The electron energy $\epsilon_a(\mathbf{k})$ and hole energies $\epsilon_{b\pm}(\mathbf{k}) = \epsilon_b(\mathbf{k} - \mathbf{Q}'_{\pm})$ correspond to three distinct bands in the I phase. In Figs. 3(b) and 3(c) for the I and C phases, the linearized, paramagnetic quasiparticle energies are plotted as dashed lines. We assume that the electron and hole Fermi velocities have the same magnitude v_F . Below the Néel temperature, the hybridized quasiparticle energies are plotted in the solid curves.

The Coulomb interaction U couples electrons on the a band with holes on the $b\pm$ bands to produce a SDW with order parameter $g > 0$. Since these quasiparticles differ by momenta \mathbf{Q}'_{\pm} , the SDW can be written as¹⁴

$$\mathbf{S}(\mathbf{r}) = -\frac{2\hbar}{U} Vg(T) \hat{\mathbf{m}} |u(\mathbf{r})|^2 \times \{\cos(\mathbf{Q}'_+ \cdot \mathbf{r} - \phi_+) + \cos(\mathbf{Q}'_- \cdot \mathbf{r} - \phi_-)\}, \quad (1)$$

where $\hat{\mathbf{m}}$ is the polarization direction and ϕ_{\pm} are arbitrary phases. A CDW with order parameter $d < 0$ is similarly produced by the Coulomb attraction U' between electrons and

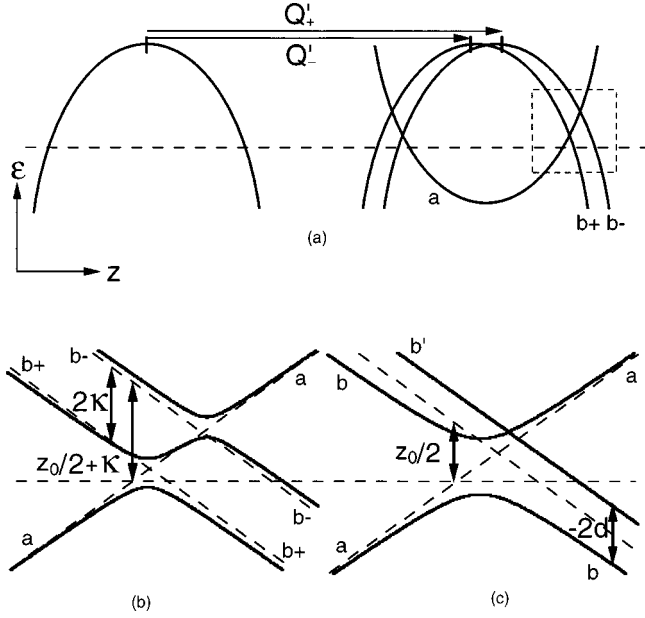


FIG. 3. (a) The electron (a) and hole (b) energies translated by the SDW wave vectors \mathbf{Q}'_{\pm} . In (b) and (c), we expand the boxed region near the Fermi energy for the quasiparticle energies above (short-dashed) and below (solid) the Néel temperature for the I and C phases. In all three figures, the chemical potential is denoted by a horizontal dashed line.

holes on the $b+$ and $b-$ bands. The momentum difference between a $b+$ and $b-$ quasiparticle is $\mathbf{Q}'_+ - \mathbf{Q}'_- = 2\mathbf{Q}'_+ - \mathbf{G} = \mathbf{G} - 2\mathbf{Q}'_-$. Hence, the CDW is the second harmonic of the SDW and takes the form

$$\varrho(\mathbf{r}) = -\frac{4}{U'} V d(T) |u(\mathbf{r})|^2 \cos[(\mathbf{Q}'_+ - \mathbf{Q}'_-) \cdot \mathbf{r} - \theta]. \quad (2)$$

In both relations, $u(\mathbf{r})$ is normalized to 1 in volume V . Because $\theta = \phi_+ - \phi_-$, the spin and charge distributions are in phase and the electron density $\varrho(\mathbf{r})$ is largest where the SDW has an antinode.¹⁵

Since the d -band Bloch wave functions are strongly peaked at the atomic sites, the maximum values of the spin and charge densities in the I phase are

$$S_0 = \frac{4\hbar g(T)}{U'} \frac{V}{N} |\cos[(\phi_+ + \phi_-)/2]|, \quad (3)$$

$$\varrho_0 = -\frac{4d(T)}{U'} \frac{V}{N}. \quad (4)$$

When $U' \rightarrow 0$, the CDW order parameter d vanishes but the ratio d/U' approaches a nonzero value. The CDW $\varrho(\mathbf{r})$ survives in the $U' \rightarrow 0$ limit due to the remnant correlation between the $b+$ and $b-$ quasiparticles induced indirectly through the SDW. As U' increases, the CDW amplitude of Eq. (4) also increases. In keeping with the scenario mentioned above, the ratio $\varrho_0(T)/S_0(T)^2$ has been observed¹¹ to be roughly independent of temperature. Within a Landau-Ginzburg expansion² of the free energy, it is readily shown that $d(T) \propto g(T)^2$ and $\varrho_0(T) \propto S_0(T)^2$.

As suggested above, the period of the SDW and CDW can be controlled by doping. Adding Mn or Fe impurities to

the Cr host reduces the size difference δ between the electron and hole Fermi surfaces and also decreases the wave vector parameter δ' . When the electron and hole Fermi surfaces are sufficiently close in size and δ is sufficiently small, $\delta' \rightarrow 0$ and the SDW becomes commensurate. To conserve charge, the CDW must disappear in the commensurate phase so that¹⁴ $\theta = \pi/2$. Experimentally,¹ Mn is much more effective than Fe at lowering the chemical potential and rendering the SDW commensurate: the triple point where the C, I, and P phases meet lies at a concentration of 0.3% Mn compared with 2.4% Fe. The effect of doping on the mismatch between the electron and hole Fermi surfaces is quantitatively gauged by the mismatch energy $z_0 = Gv_F\delta/\sqrt{3}$, which vanishes in the limit of equally sized Fermi surfaces with $\mathbf{Q}_{\pm} = \mathbf{G}/2$ and $\delta = 0$. For pure Cr, photoemission measurements¹⁶ indicate that $z_0 \approx 500$ meV.

The size difference between the electron and hole Fermi surfaces has important physical consequences in both the I and C phases. For either phase, the larger size of the hole Fermi surface implies that some of the b holes cannot be paired with a electrons in the SDW condensate. At zero temperature, it is easy to show that $\rho_{eh}z_0/2$ of the holes will be unpaired when $U' = 0$.

Despite its usefulness, the physical significance of the three-band model was questioned by Fenton and Leavens.¹⁷ Their reservations can be summarized as follows. Mathematically, the three-band model converts a system consisting of two Fermi surfaces into one with three different energy bands. In the C phase, the two hole energies $\epsilon_{b+}(\mathbf{k})$ and $\epsilon_{b-}(\mathbf{k})$ coincide above T_N . But as suggested by the solid curves of Fig. 3(c), three distinct bands of quasiparticles appear below the Néel temperature. Viewed as an artifact of the three-band model in the C limit, this suggests that the three-band model can only provide physically significant results in the I phase and cannot be used to evaluate the IC or PC phase boundaries.

This raises some fundamental questions about the validity of the three-band model in the study of Cr alloys. In particular, what is the justification for the three-band model even in the I phase? Does the three-band model correctly interpolate between the C and I phases? Since our earlier prediction¹⁴ of a first-order PC transition was based on the three-band model, can it be trusted?

In this paper, we resolve those questions. First, we provide a justification for the three-band model in the I phase of Cr alloys. Section II shows that the three-band model may be derived by ignoring harmonics above the CDW and by neglecting terms that use the Coulomb interactions to convert a $b\pm$ quasiparticle into a $b\mp$ quasiparticle. Second, we reconcile the three-band model with an ‘‘exact’’ RPA treatment of the C phase. In Sec. III, we prove that the three bands of quasiparticles obtained from the C limit of the three-band model can be collapsed into two bands, with the hole band shifted downwards in energy by d . The free energy of the three-band model reduces to the ‘‘exact’’ C free energy provided that the Coulomb interaction U' is suitably redefined. Finally, we clarify the significance of the Coulomb energy U' within the C phase. Section IV demonstrates that the energy shift of the hole band is caused by the transfer of electrons from the reservoir bands to the nested a and b bands. A Landau-Ginzburg expansion is used to find the

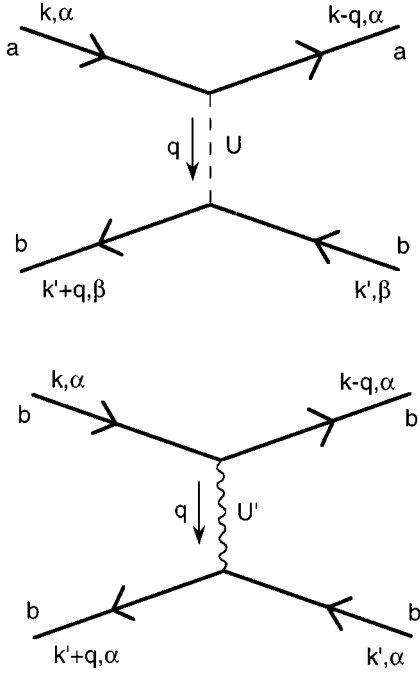


FIG. 4. The Coulomb interactions that contribute to the Hamiltonian of Eq. (5).

critical value of U' that produces a first-order PC transition. Hence, we argue that the first-order PC transition in CrFe and CrSi alloys is preceded by the growth of a large CDW in the I phase of those alloys. As discussed in the conclusion, this prediction can be tested experimentally. Formal results are summarized in the three Appendixes.

II. THREE-BAND MODEL FOR COUPLED SPIN- AND CHARGE-DENSITY WAVES

In the I phase, the three-band model has a rather natural derivation. Our starting point is the Hamiltonian

$$\begin{aligned}
 H = & \sum_{\mathbf{k}, \sigma} \{ \epsilon_a(\mathbf{k}) a_{\mathbf{k}\sigma}^\dagger a_{\mathbf{k}\sigma} + \epsilon_b(\mathbf{k}) b_{\mathbf{k}\sigma}^\dagger b_{\mathbf{k}\sigma} \} \\
 & + \frac{1}{V} \sum_{\mathbf{q}, \mathbf{k}, \mathbf{k}', \alpha, \beta} U(\mathbf{q}) a_{\mathbf{k}\alpha}^\dagger b_{\mathbf{k}'\beta}^\dagger b_{\mathbf{k}'+\mathbf{q}\beta} a_{\mathbf{k}-\mathbf{q}\alpha} \\
 & + \frac{1}{2V} \sum_{\mathbf{q}, \mathbf{k}, \mathbf{k}', \alpha} U'(\mathbf{q}) b_{\mathbf{k}\alpha}^\dagger b_{\mathbf{k}'\alpha}^\dagger b_{\mathbf{k}'+\mathbf{q}\alpha} b_{\mathbf{k}-\mathbf{q}\alpha}, \quad (5)
 \end{aligned}$$

where $U(\mathbf{q})$ and $U'(\mathbf{q})$ are the Coulomb energies responsible for the SDW and CDW, respectively. While U acts between both parallel- and antiparallel-spin electron-hole pairs on the a and b bands, U' acts between parallel-spin electron-hole pairs on the b band. These interactions are pictured in Fig. 4. For simplicity, we have not included the Coulomb interaction between electrons and holes on the a Fermi surface. Such an interaction is not required to obtain a CDW and would only complicate our model without changing any of its conclusions. Nor have we explicitly included the contributions of the reservoir electrons. Except where noted, we shall assume that the reservoir is infinite so that the chemical potential is not affected by the formation of the SDW condensate.

The imaginary time operators $A(\tau)$ are defined in the usual fashion as $A(\tau) = \exp(\tau H) A \exp(-\tau H)$, where τ is restricted between 0 and $\beta = 1/T$. Using the Hamiltonian above and the fermion commutation relations, we find

$$\frac{da_{\mathbf{k}\alpha}(\tau)}{d\tau} = -\epsilon_a(\mathbf{k}) a_{\mathbf{k}\alpha} - \frac{1}{V} \sum_{\mathbf{q}, \mathbf{k}', \beta} U(\mathbf{q}) b_{\mathbf{k}'\beta}^\dagger b_{\mathbf{k}'+\mathbf{q}\beta} a_{\mathbf{k}-\mathbf{q}\alpha}, \quad (6a)$$

$$\begin{aligned}
 \frac{db_{\mathbf{k}\alpha}(\tau)}{d\tau} = & -\epsilon_b(\mathbf{k}) b_{\mathbf{k}\alpha} - \frac{1}{V} \sum_{\mathbf{q}, \mathbf{k}', \beta} U(\mathbf{q}) a_{\mathbf{k}'\beta}^\dagger a_{\mathbf{k}'+\mathbf{q}\beta} b_{\mathbf{k}-\mathbf{q}\alpha} \\
 & - \frac{1}{V} \sum_{\mathbf{q}, \mathbf{k}'} U'(\mathbf{q}) b_{\mathbf{k}'\alpha}^\dagger b_{\mathbf{k}'+\mathbf{q}\alpha} b_{\mathbf{k}-\mathbf{q}\alpha}. \quad (6b)
 \end{aligned}$$

Although not explicitly indicated, all operators on the right-hand sides of these relations are functions of τ .

We now formulate the equations of motion for the imaginary time Green's functions

$$G(\mathbf{k}, \tau)_{\alpha\beta, aa} = -\langle T_\tau a_{\mathbf{k}\alpha}(\tau) a_{\mathbf{k}\beta}^\dagger(0) \rangle, \quad (7a)$$

$$G(\mathbf{k}, \tau)_{\alpha\beta, ab\pm} = -\langle T_\tau a_{\mathbf{k}\alpha}(\tau) b_{\mathbf{k}\beta}^{(\pm)\dagger}(0) \rangle, \quad (7b)$$

$$G(\mathbf{k}, \tau)_{\alpha\beta, b\pm b\pm} = -\langle T_\tau b_{\mathbf{k}\alpha}^{(\pm)}(\tau) b_{\mathbf{k}\beta}^{(\pm)\dagger}(0) \rangle, \quad (7c)$$

$$G(\mathbf{k}, \tau)_{\alpha\beta, b\pm b\mp} = -\langle T_\tau b_{\mathbf{k}\alpha}^{(\pm)}(\tau) b_{\mathbf{k}\beta}^{(\mp)\dagger}(0) \rangle, \quad (7d)$$

$$G(\mathbf{k}, \tau)_{\alpha\beta, b\pm a} = -\langle T_\tau b_{\mathbf{k}\alpha}^{(\pm)}(\tau) a_{\mathbf{k}\beta}^\dagger(0) \rangle, \quad (7e)$$

where T_τ is the time-ordering operator and the $b_{\mathbf{k}\alpha}^{(\pm)}$ operators are defined by

$$b_{\mathbf{k}\alpha}^{(\pm)} = b_{\mathbf{k}-\mathbf{Q}'_{\mp}, \alpha}. \quad (8)$$

Despite the experimental evidence for their existence,¹ higher harmonics of the spin- and charge-density waves are ignored. For example, we set $\langle T_\tau a_{\mathbf{k}\alpha}(\tau) b_{\mathbf{k}+2\mathbf{Q}'_{+}-\mathbf{Q}'_{-}\beta}^\dagger(0) \rangle$ and $\langle T_\tau b_{\mathbf{k}-2\mathbf{Q}'_{+}\alpha}(\tau) b_{\mathbf{k}-2\mathbf{Q}'_{-}\beta}^\dagger(0) \rangle$ to zero. These ‘‘off-diagonal’’ Green's functions correspond to the third and fourth harmonics of the SDW, with the latter also corresponding to the second harmonic of the CDW.

Using Eqs. (6a) and (6b) and applying the RPA to the two-particle correlation functions, we obtain the equations of motion in Appendix A. The $ab\pm$ and $b\pm a$ Green's functions are chosen¹⁸ to have spin symmetry $\hat{\mathbf{m}} \cdot \sigma_{\alpha\beta}$ while all other Green's functions including the $b\pm b\mp$ components are proportional to the unit matrix $\delta_{\alpha\beta}$ in spin space. We also introduce the self-energies

$$\Delta_{\alpha\beta}^{(\pm)}(\mathbf{k}) = -\frac{1}{V} T \sum_{\mathbf{k}', l} U(\mathbf{k}-\mathbf{k}') G(\mathbf{k}', i\nu_l)_{\alpha\beta, ab\pm}, \quad (9a)$$

$$\bar{\Delta}_{\alpha\beta}^{(\pm)}(\mathbf{k}) = -\frac{1}{V} T \sum_{\mathbf{k}', l} U(\mathbf{k}-\mathbf{k}') G(\mathbf{k}', i\nu_l)_{\alpha\beta, b\pm a}, \quad (9b)$$

$$\Gamma_{\alpha\beta}^{(\pm\mp)}(\mathbf{k}) = -\frac{1}{V} T \sum_{\mathbf{k}', l} U'(\mathbf{k}-\mathbf{k}') G(\mathbf{k}', i\nu_l)_{\alpha\beta, b\pm b\mp}, \quad (10)$$

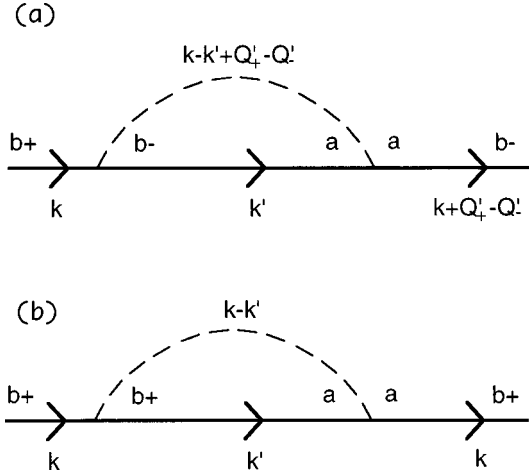


FIG. 5. Two terms that contribute to the equation of motion for $G(\mathbf{k}, \tau)_{b+b+}$. Within the three-band model, the first term is neglected and the second is retained.

where the Fourier-transformed Green's functions are defined by Eq. (A2) in Appendix A. Due to the spin symmetries of the Green's functions, we may write $\Delta_{\alpha\beta}^{(\pm)} = \Delta^{(\pm)} \hat{\mathbf{m}} \cdot \boldsymbol{\sigma}_{\alpha\beta}$, $\bar{\Delta}_{\alpha\beta}^{(\pm)} = \bar{\Delta}^{(\pm)} \hat{\mathbf{m}} \cdot \boldsymbol{\sigma}_{\alpha\beta}$, and $\Gamma_{\alpha\beta}^{(\pm\mp)} = \Gamma^{(\pm\mp)} \delta_{\alpha\beta}$.

Besides neglecting higher harmonics, the three-band model also requires that we neglect terms like

$$\frac{1}{V} T \sum_{\mathbf{k}', l'} U(\mathbf{k} - \mathbf{k}' + \mathbf{Q}'_+ - \mathbf{Q}'_-) G(\mathbf{k}', i\nu_l)_{b-a} \times G(\mathbf{k} + \mathbf{Q}'_+ - \mathbf{Q}'_-, i\nu_l)_{ab-}, \quad (11)$$

which enters the equation of motion for $G(\mathbf{k}, \tau)_{b+b+}$. By contrast, the retained term can be written as

$$\frac{1}{V} T \sum_{\mathbf{k}', l'} U(\mathbf{k} - \mathbf{k}') G(\mathbf{k}', i\nu_l)_{b+a} \times G(\mathbf{k}, i\nu_l)_{ab+}. \quad (12)$$

These two terms are represented by the Feynman diagrams in Fig. 5. Since the momentum of a $b\pm$ quasiparticle is shifted by \mathbf{Q}'_{\mp} , both diagrams carry the same incoming and outgoing momentum $\mathbf{k} - \mathbf{Q}'_{-}$.

The neglected term differs from the retained one in two ways. Equation (11) uses the momentum removed by the Coulomb energy U to convert an incoming $b+$ quasiparticle into an intermediate $b-$ quasiparticle. As shown in Fig. 3(a), the energy of a $b+$ ($b-$) quasiparticle lies close to the chemical potential only on the right-hand (left-hand) side of the a Fermi surface. So the momentum $\mathbf{k} - \mathbf{k}' + \mathbf{Q}'_+ - \mathbf{Q}'_-$ removed by the Coulomb interaction must be of order $2k_F$. In the retained term of Fig. 5(b), on the other hand, the b quasiparticle remains in the same band so that the Coulomb interaction carries a much smaller momentum. In Fig. 5(a), an intermediate a quasiparticle receives the momentum transferred by the Coulomb interaction to achieve a final momentum of $\mathbf{k} + \mathbf{Q}'_+ - \mathbf{Q}'_-$. But if the exiting $b-$ quasiparticle lies near the Fermi energy, then the intermediate a quasiparticle would lie an energy $z_0 \approx 500$ meV away. Therefore, the contribution of Fig. 5(a) is of order $T/z_0 \approx 1/20$ times smaller than the contribution of Fig. 5(b).

To complete the three-band model, we expand the Coulomb interactions $U(\mathbf{k} - \mathbf{k}')$ and $U'(\mathbf{k} - \mathbf{k}')$ in cubic harmonics. Only the lowest-order, constant terms are retained. Consequently, the self-energies $\Delta^{(\pm)}$ and $\Gamma^{(\pm\mp)}$ are independent of momentum. The identity $\theta = \phi_+ - \phi_-$ follows from the self-consistent relations of Eqs. (9a) and (10). With the definitions $\Delta^{(\pm)} = g \exp(i\phi_{\pm})$, $\bar{\Delta}^{(\pm)} = g \exp(-i\phi_{\pm})$, and $\Gamma^{(\pm\mp)} = d \exp(\mp i\theta)$, the self-consistent relations may be rewritten as

$$g = -\frac{U}{2V} T \sum_{\mathbf{k}, l} g \frac{2i\nu_l - \epsilon_{b+}(\mathbf{k}) - \epsilon_{b-}(\mathbf{k}) + 2d}{D_3(\mathbf{k}, i\nu_l)}, \quad (13)$$

$$d = -\frac{U'}{V} T \sum_{\mathbf{k}, l} \frac{[i\nu_l - \epsilon_a(\mathbf{k})]d + g^2}{D_3(\mathbf{k}, i\nu_l)}, \quad (14)$$

with denominator

$$D_3(\mathbf{k}, i\nu_l) = [i\nu_l - \epsilon_a(\mathbf{k})][i\nu_l - \epsilon_{b+}(\mathbf{k})][i\nu_l - \epsilon_{b-}(\mathbf{k}) - g^2[2i\nu_l - \epsilon_{b+}(\mathbf{k}) - \epsilon_{b-}(\mathbf{k}) + 2d] - d^2[i\nu_l - \epsilon_a(\mathbf{k})]. \quad (15)$$

We also define the dimensionless coupling constants $\lambda = \rho_{\text{eh}}U/8$ and $\lambda' = \rho_{\text{eh}}U'/8$. In both self-consistent relations, the sum over ν_l must be performed prior to the summation over \mathbf{k} . Reversing the order of the summations in Eq. (14) for d would generate a term $2\lambda'd$ on the right-hand side.

The free-energy difference ΔF_3 of the three-band model is obtained by integrating Eqs. (13) and (14) with the result

$$\Delta F_3(g, d, \delta') = \rho_{\text{eh}} \left\{ \frac{g^2}{2\lambda} + \frac{d^2}{4\lambda'} (1 - 2\lambda') - \frac{2T}{V\rho_{\text{eh}} l, \mathbf{k}} \sum \ln \left| \frac{D_3(g, d, \delta', \mathbf{k}, i\nu_l)}{D_3(0, 0, \delta', \mathbf{k}, i\nu_l)} \right| \right\}. \quad (16)$$

In order to reverse the summations over ν_l and \mathbf{k} , a term $-\rho_{\text{eh}}d^2/2$ was added to the free energy. As required, minimization of $\Delta F_3(g, d, \delta')$ with respect to g and d reproduces Eqs. (13) and (14). The ordering wave vectors \mathbf{Q}_{\pm} are obtained by minimizing $\Delta F_3(g, d, \delta')$ with respect to δ' . Despite the utility of such a procedure in Fig. 2, the free energy ΔF_3 cannot be separated into contributions ΔF_+ and ΔF_- from nesting on one side or the other of the two Fermi surfaces. Instead, the energy mismatch on one side of the Fermi surface directly affects the nesting on the other side.

To evaluate the Green's functions and self-consistent equations, we must specify the paramagnetic energies $\epsilon_a(\mathbf{k})$, $\epsilon_{b+}(\mathbf{k})$, and $\epsilon_{b-}(\mathbf{k})$. Assuming that the ordering wave vectors \mathbf{Q}_{\pm} lie along the \mathbf{z} axis, the quasiparticle energies may be linearized close to each face of the octahedral Fermi surface with normal $\hat{\mathbf{n}}$. The linearized energies are given by $\epsilon_a(\mathbf{k}) = z(\mathbf{k})$, $\epsilon_{b+}(\mathbf{k}) = z_0/2 - \kappa \text{sgn}(k_z) - z(\mathbf{k})$, and $\epsilon_{b-}(\mathbf{k}) = z_0/2 + \kappa \text{sgn}(k_z) - z(\mathbf{k})$, where $z(\mathbf{k}) = v_F(\mathbf{k} \cdot \hat{\mathbf{n}} - k_F)$ and $\kappa = z_0\delta'/2\delta$. If the ordering and nesting wave vectors coincided with $\delta' = \delta$, then the mismatch between the a and $b+$ ($k_z < 0$) or $b-$ ($k_z > 0$) energies at the Fermi momentum would equal z_0 . In the C state with $\delta' = 0$, the linearized $\epsilon_{b+}(\mathbf{k})$ and $\epsilon_{b-}(\mathbf{k})$ energies are identical.

The hybridized quasiparticle energies $\epsilon(\mathbf{k})$ in Figs. 3(b) and 3(c) are obtained from the zeroes of the denominator $D_3(\mathbf{k}, \epsilon)$. In the C phase with $\delta' = 0$, this produces three bands with energies

$$\epsilon_{ab}(\mathbf{k}) = \frac{z_0}{4} + \frac{d}{2} - \sqrt{2g^2 + (z - z_0/4 - d/2)^2}, \quad (17a)$$

$$\epsilon_{ba}(\mathbf{k}) = \frac{z_0}{4} + \frac{d}{2} + \sqrt{2g^2 + (z - z_0/4 - d/2)^2}, \quad (17b)$$

$$\epsilon_{b'}(\mathbf{k}) = -z + \frac{z_0}{2} - d. \quad (17c)$$

Both the survival of three bands in the C limit and the appearance of a linear b' band are rather puzzling consequences of the three-band model.

To set the stage for future discussion, one additional parameter must be defined. The self-consistent relation for g given by Eq. (13) contains a logarithmically divergent integral over the energy z . To regulate this divergence, we impose the cutoff ϵ_0 , which is assumed to be much smaller than the Fermi energy but much larger than the Néel temperature. This cutoff only appears implicitly in the Néel temperature

$$T_N^* = \frac{2\gamma}{\pi} \epsilon_0 e^{-1/2\lambda} \approx 100 \text{ meV} \quad (18)$$

of a perfectly nested C alloy with $z_0 = 0$. Here, $\ln \gamma \approx 0.577$ is Euler's constant. When $U' = 0$, the energy mismatch at the triple point¹⁹ is given in units of T_N^* by $z_0 = 4.276 T_N^*$.

III. TWO- AND THREE-BAND MODELS IN THE C PHASE

The RPA equations of motion for the Green's functions in the C phase are summarized in Appendix B. Using the definitions $\Delta = \sqrt{2}g \exp(i\phi)$, $\bar{\Delta} = \sqrt{2}g \exp(-i\phi)$, and $D = d$, these coupled equations have the solutions

$$G(\mathbf{k}, i\nu_l)_{aa} = \frac{i\nu_l - \epsilon_{b+}(\mathbf{k}) - d}{D_2(\mathbf{k}, i\nu_l)}, \quad (19a)$$

$$G(\mathbf{k}, i\nu_l)_{ba} = \frac{\sqrt{2}g e^{-i\phi}}{D_2(\mathbf{k}, i\nu_l)}, \quad (19b)$$

$$G(\mathbf{k}, i\nu_l)_{ab} = \frac{\sqrt{2}g e^{i\phi}}{D_2(\mathbf{k}, i\nu_l)}, \quad (19c)$$

$$G(\mathbf{k}, i\nu_l)_{bb} = \frac{i\nu_l - \epsilon_a(\mathbf{k})}{D_2(\mathbf{k}, i\nu_l)}, \quad (19d)$$

with denominator

$$D_2(\mathbf{k}, i\nu_l) = [i\nu_l - \epsilon_a(\mathbf{k})][i\nu_l - \epsilon_{b+}(\mathbf{k}) - d] - 2g^2. \quad (20)$$

The zeroes of $D_2(\mathbf{k}, \epsilon)$ coincide with the solutions $\epsilon_{ab}(\mathbf{k})$ and $\epsilon_{ba}(\mathbf{k})$ of Eqs. (17a) and (17b). But unlike the C limit of the three-band model, only two bands appear in an "exact" solution of the RPA equations in the C phase and there is no sign of the third b' band. A factor of $\sqrt{2}$ was introduced into

the definition of Δ so that the energy gap $2\sqrt{2}g$ between the ab and ba bands is the same as in the C limit of the three-band model.

Once again, we expand the Coulomb interactions $U(\mathbf{q})$ and $U'(\mathbf{q})$ in terms of cubic harmonics and keep only the lowest-order, constant term in the self-consistent relations for g and d given by Eqs. (B2a) and (B2b) in Appendix B. Upon integrating these relations, we find that the C free energy can be written

$$\begin{aligned} \Delta F_2(g, d) = \rho_{\text{eh}} \left\{ \frac{g^2}{2\lambda} + \frac{d^2}{8\lambda'} - \frac{2T}{V\rho_{\text{eh}}} \right. \\ \left. \times \sum_{l, \mathbf{k}} \left[\ln \left| \frac{D_2(g, d, \mathbf{k}, i\nu_l)}{D_2(0, 0, \mathbf{k}, i\nu_l)} \right| + \frac{d}{i\nu_l - \epsilon_b(\mathbf{k})} \right] \right\}. \end{aligned} \quad (21)$$

Unlike the summations in ΔF_3 for the I phase, the \mathbf{k} and ν_l sums in ΔF_2 may be interchanged without consequence.

At first sight, the free energies $\Delta F_3(g, d, \delta' = 0)$ and $\Delta F_2(g, d)$ seem irreconcilable. But the C limit of ΔF_3 can be simplified using the factorization

$$\begin{aligned} D_3(\mathbf{k}, i\nu_l) = \{ [i\nu_l - \epsilon_a(\mathbf{k})][i\nu_l - \epsilon_{b+}(\mathbf{k}) - d] - 2g^2 \} \\ \times [i\nu_l - \epsilon_{b+}(\mathbf{k}) + d] \\ = D_2(\mathbf{k}, i\nu_l)[i\nu_l - \epsilon_{b+}(\mathbf{k}) + d]. \end{aligned} \quad (22)$$

Then $\Delta F_3(g, d, \delta' = 0)$ contains the contribution

$$\begin{aligned} \sum_{l, \mathbf{k}} \ln \left| \frac{i\nu_l - \epsilon_{b+}(\mathbf{k}) + d}{i\nu_l - \epsilon_{b+}(\mathbf{k})} \right| = \sum_{l, \mathbf{k}} \text{Re} \left\{ \frac{d}{i\nu_l - \epsilon_{b+}(\mathbf{k})} \right. \\ \left. - \frac{1}{2} \left(\frac{d}{i\nu_l - \epsilon_{b+}(\mathbf{k})} \right)^2 \right. \\ \left. + \frac{1}{3} \left(\frac{d}{i\nu_l - \epsilon_{b+}(\mathbf{k})} \right)^3 - \dots \right\}, \end{aligned} \quad (23)$$

in which the \mathbf{k} sum is performed first. It is easy to show that every term in this summation vanishes. Hence, we can rewrite the C free energy of the three-band model as

$$\begin{aligned} \Delta F_3(g, d, \delta' = 0) = \rho_{\text{eh}} \left\{ \frac{g^2}{2\lambda} + \frac{d^2}{4\lambda'} (1 - 2\lambda') - \frac{2T}{V\rho_{\text{eh}}} \right. \\ \left. \times \sum_{l, \mathbf{k}} \left[\ln \left| \frac{D_2(g, d, \mathbf{k}, i\nu_l)}{D_2(0, 0, \mathbf{k}, i\nu_l)} \right| \right. \right. \\ \left. \left. + \frac{d}{i\nu_l - \epsilon_b(\mathbf{k})} \right] \right\}, \end{aligned} \quad (24)$$

which is identical to $\Delta F_2(g, d)$ except for a change in the coupling constant λ' .

If the coupling constant in the three-band model is denoted by λ'_3 , then the two- and three-band models for the C phase are equivalent provided that

$$\lambda'_2 = \frac{1}{2} \frac{\lambda'_3}{1 - 2\lambda'_3}. \quad (25)$$

Within the three-band model, λ'_3 is restricted to the range $0 \leq \lambda'_3 \leq \frac{1}{2}$. As $\lambda'_3 \rightarrow \frac{1}{2}$, the ICDW becomes unstable with a divergent amplitude. In an “exact” RPA treatment of the C phase, however, no such instability occurs. We see from Eq. (25) that the $\lambda'_3 \rightarrow \frac{1}{2}$ limit corresponds to the $\lambda'_2 \rightarrow \infty$ limit within the two-band model. This suggests that the three-band model compensates for the neglect of higher harmonics and the absence of terms like Eq. (11) by introducing an instability in λ'_3 . Such an instability should disappear in an “exact” treatment of the I phase within the RPA. But due to the different momentum dependences of the Coulomb energies in Eq. (11) and Eq. (12), there is no easy way to retain the contribution of terms like Eq. (11).

These results suggest that there are two ways to consistently apply the three-band model to both the C and I phases. The first is to simply use Eqs. (16) and (24) with the coupling constant λ'_3 . These two relations guarantee that the free energy is continuous across a second-order IC phase transition with the same order parameters g and d on both sides. An alternate method is to use Eq. (25) to introduce the coupling constant λ'_2 into both Eqs. (16) and (24). The ICDW instability as $\lambda'_3 \rightarrow \frac{1}{2}$ is then replaced by an instability as $\lambda'_2 \rightarrow \infty$. In these two limits, it can be shown¹⁴ that the C phase obtains a lower free energy than the I phase for all values of the mismatch energy z_0 .

Within either the two- or three-band models, it is straightforward to evaluate the order parameters g and d at $T=0$ in the C phase. We find that

$$g(0) = \frac{\pi}{\gamma\sqrt{2}} T_N^* \approx 1.247 T_N^*, \quad (26)$$

$$d(0) = -\frac{\lambda'_2 z_0}{2(1+\lambda'_2)} < 0. \quad (27)$$

The last relation implies that the downward shift in the ab and ba bands only occurs when the mismatch energy z_0 is nonzero. Notice from Fig. 3(c) that the midpoint between the ab and ba bands lies $z_0/4 + d/2$ above the chemical potential. As $\lambda'_2 \rightarrow \infty$, Eq. (27) implies that $d(0) \rightarrow -z_0/2$ so that the energy bands lie symmetrically on either side of the chemical potential. The significance of this result will be discussed in the next section.

IV. FIRST-ORDER PC TRANSITION

Our final task is to clarify the physics of the first-order PC transition produced by the Coulomb interaction U' in the C phase of the SDW. The existence of such a first-order transition can be easily demonstrated by performing a Landau-Ginzburg expansion of either free energy ΔF_2 or ΔF_3 . Expanded in powers of g and d , $\Delta F_2(g, d)$ can be written as

$$\frac{\Delta F_2(g, d)}{\rho_{eh} T_N^{*2}} = A \left(\frac{g}{T_N^*} \right)^2 + B \left(\frac{g}{T_N^*} \right)^4 + C \left(\frac{d}{T_N^*} \right) + D \left(\frac{d}{T_N^*} \right)^2 + E \left(\frac{g}{T_N^*} \right)^2 \left(\frac{d}{T_N^*} \right) + \dots, \quad (28)$$

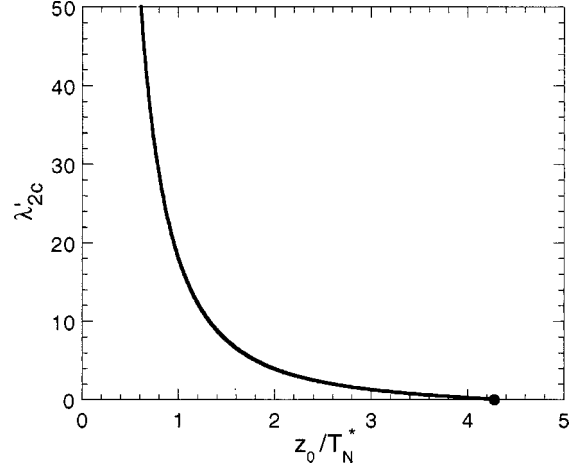


FIG. 6. The critical value of λ'_2 versus the energy mismatch z_0/T_N^* in the C phase. The black dot denotes the triple point.

with coefficients given in Appendix C. To express the free energy as a function of a single variable, we require that the derivative of ΔF_2 with respect to d must vanish. Since the linear coefficient C vanishes, we find that to lowest order in g/T_N^* ,

$$\frac{d}{T_N^*} = -\frac{E}{2D} \left(\frac{g}{T_N^*} \right)^2. \quad (29)$$

Substituting this expression back into Eq. (28) for $\Delta F_2(g, d)$, we obtain the expansion

$$\frac{\Delta F_2(g, d)}{\rho_{eh} T_N^{*2}} = A' \left(\frac{g}{T_N^*} \right)^2 + B' \left(\frac{g}{T_N^*} \right)^4 + \dots, \quad (30)$$

$$A' = A, \quad (31)$$

$$B' = B - \frac{E^2}{4D} = B - 2\lambda'_2 E^2, \quad (32)$$

which uses our result $D = 1/(8\lambda')$.

The phase transition becomes first order when the g^2 and g^4 coefficients change sign. So the threshold value of λ'_2 is given by

$$\lambda'_{2c} = \frac{S_3^2}{S_2}, \quad (33)$$

$$S_2 = \sum_{n=0}^{\infty} \text{Im} \left(\frac{1}{X_n^2} \right), \quad (34a)$$

$$S_3 = \sum_{n=0}^{\infty} \text{Re} \left(\frac{1}{X_n^3} \right), \quad (34b)$$

$$X_n = n + \frac{1}{2} + i \frac{z_0}{8\pi T_N}. \quad (35)$$

The critical value λ'_{2c} is plotted versus the normalized energy mismatch z_0/T_N^* in Fig. 6. When the Fermi-surface nesting is perfect with $z_0=0$, then $S_2=0$ so that $\lambda'_{2c} = \infty$ and the PC transition is always second order. At the triple point,¹⁹ how-

ever, $S_3=0$ so $\lambda'_{2c}=0$. Then the PC transition is first order for any nonzero coupling constant λ'_2 .

Our assumption of an infinite electron reservoir implies that the chemical potential is not depressed by the formation of the SDW. In order to keep the chemical potential fixed, electrons must transfer from the reservoir bands to the nested a and b bands below T_N . The change in occupation of the a and b bands is given by

$$\Delta\rho_{aa}(T) = \frac{2T}{V} \sum_{\mathbf{k},l} \left\{ G(\mathbf{k}, i\nu_l)_{\uparrow\uparrow,aa} - \frac{1}{i\nu_l - \epsilon_a(\mathbf{k})} \right\}, \quad (36)$$

$$\Delta\rho_{bb}(T) = \frac{2T}{V} \sum_{\mathbf{k},l} \left\{ G(\mathbf{k}, i\nu_l)_{\uparrow\uparrow,bb} - \frac{1}{i\nu_l - \epsilon_{b+}(\mathbf{k})} \right\}. \quad (37)$$

Due to their spin symmetries, the contributions of the off-diagonal ab and ba matrix elements vanish. The above relations imply that

$$\Delta\rho_{aa}(T) = \Delta\rho_{bb}(T) = -\frac{1}{4} \rho_{eh} \frac{d(T)}{\lambda'_2} > 0, \quad (38)$$

so there is a net transfer of electrons from the reservoir bands to the nested a and b bands.

At zero temperature, Eq. (27) implies that the total number of transferred electrons is given by

$$\Delta\rho_{aa}(0) + \Delta\rho_{bb}(0) = \frac{1}{4} \rho_{eh} z_0 \frac{1}{1 + \lambda'_2}. \quad (39)$$

But at $T=0$, the chemical potential lies

$$\frac{z_0}{4} + \frac{d(0)}{2} = \frac{1}{2} z_0 \frac{1}{1 + \lambda'_2} \quad (40)$$

above the midpoint between the ab and ba bands. Consequently, the electrons transferred from the reservoir exactly balance the excess holes remaining on the b Fermi surface.

The transferred electrons $\Delta\rho_{bb}(T)$ interact electrostatically with the original b electrons through the U' term in the Hamiltonian of Eq. (5). Due to the net excess of holes on the nested a and b bands, the ab and ba bands are shifted *downward* in energy by the attraction between the transferred electrons and the excess holes. Indeed, we may write the energy shift $d(T)$ of the b band as

$$d(T) = -\frac{1}{2} U' \Delta\rho_{bb}(T), \quad (41)$$

where the factor of $\frac{1}{2}$ reflects the counting of both spin states in $\Delta\rho_{bb}(T)$ (U' only couples like spins). So as λ'_2 increases, the energy shift also grows. This brings the chemical potential closer to the midpoint between the ab and ba bands, which in turn lowers the number of transferred electrons $\Delta\rho_{bb}(T)$ from the reservoir bands. We emphasize that the downward shift in energy of the ab and ba bands is produced by the *change* in electrostatic energy induced by the transferred electrons. Such a shift does not occur in a BCS superconductor because the number of \uparrow and \downarrow electrons is the same. Hence, the formation of the BCS condensate does not initiate the transfer of electrons from other bands.

V. DISCUSSION AND CONCLUSION

This paper has served three different purposes. First, we have justified the three-band model for an I system of coupled spin- and charge-density waves. In addition to neglecting higher harmonics, the three-band model also neglects terms that use the Coulomb interactions to change a $b \pm$ quasiparticle into a $b \mp$ quasiparticle. Such terms were shown to be of order $T/z_0 \approx 1/20$ compared to the terms that are retained.

Our second goal was to show that the three-band model reduces to the correct C limit. Due to the approximations made within the I phase, the Coulomb interaction constant U' of the three-band model has an exaggerated effect and the thermodynamics becomes singular as $\lambda' = \rho_{eh} U' / 8 \rightarrow \frac{1}{2}$. In an exact treatment of the I phase, the singularity at $\lambda' = \frac{1}{2}$ would be replaced by one at $\lambda' = \infty$. With the substitution of λ'_3 by $\lambda'_2 = \lambda'_3 / [2(1 - 2\lambda'_3)]$, the singularity at $\lambda'_3 = \frac{1}{2}$ is removed and the three-band model correctly interpolates between the C and I phases.

Finally, we have shown that a first-order PC transition is caused by the redistribution of electrons between the nested and non-nested bands. The Coulomb attraction between the b -band holes and the electrons transferred from the reservoir bands lowers the energy of the b band. This rearrangement of electronic charge may be responsible for the tetragonal lattice distortion in γ -Mn alloys, which supports a CSDW.²⁰ When the electron reservoir is infinite and the chemical potential is fixed, the electrostatic interaction U' always favors a first-order PC transition in the vicinity of the triple point.

However, a finite electron reservoir may defeat this first-order PC transition for small λ' . Qualitatively, this may be understood as follows. If ρ_r is finite, then the reservoir will not transfer as many electrons to the nested bands.²¹ Hence, the shift in the b -band energy becomes smaller as the size of the reservoir decreases. By introducing an additional term into the Landau-Ginzburg coefficient B' ,²² the finite reservoir produces a nonzero threshold λ'_{2c} even at the triple point.

This competition between the electron reservoir and the electrostatic coupling U' may explain the absence of a first-order PC transition in CrMn alloys: the reservoir density-of-states ρ_r and the coupling constant λ' may be too small to support a first-order PC transition. By contrast, the relatively localized Fe electrons may act to enhance the electron reservoir through a magnetostrictive effect.³

As shown by Nakanishi and Kasuya,³ the change in mismatch energy $\Delta z_0 = \eta \Delta V / V$ with the volume change ΔV acts to enhance the electron reservoir. Formally, the magnetostriction $1/a \equiv \rho_{eh} \eta^2 / \mathcal{B}$ (\mathcal{B} is the Bulk modulus) plays an identical role to the coupling constant λ'_2 in the Landau-Ginzburg coefficient B' of Eq. (32). So magnetostriction also favors the C phase and drives a first-order transition. While active in other alloys as well, magnetostriction may be particularly important in CrFe alloys due to the extra electrons on each Fe impurity. For any alloy, $1/\sqrt{a}$ is predicted to decrease linearly with the energy mismatch z_0 . The magnetostriction $1/a$ can be absorbed into an effective reservoir with power

$$\frac{1}{\rho_r+1} = \frac{1}{\rho_{r0}+1} - \frac{1}{a}, \quad (42)$$

where ρ_{r0} is the reservoir power in the absence of magnetostriction.

Although appealing, this explanation has several problems. First, the effective reservoir power of the I phase becomes singular as a passes through $\rho_{r0}+1$. Even more troubling, the negative electron reservoir with $a < \rho_{r0}+1$ and $\rho_r < 0$ has no physical interpretation. It seems much more plausible that magnetostriction works in tandem with the coupling λ'_2 by enhancing the reservoir power. To ensure that the effective reservoir power ρ_r remains positive, the magnetostriction a must be restricted to values greater than $\rho_{r0}+1$. Even a modest magnetostriction would substantially increase the effective reservoir power ρ_r . Although magnetostriction cannot alone induce a first-order PC transition, it does act to diminish the critical value $\lambda'_{2c}(\rho_r)$.

In retrospect, the equivalence of the two- and three-band models in the C phase is not so surprising. The interacting density of states $\rho(\epsilon)$ derived from the three-band model²³ in the C limit is identical to the density of states obtained from a two-band model with a shifted chemical potential. As expected, the linear b' band makes no contribution. When the IC transition is second order, Fishman and Viswanath²³ demonstrated that $\rho(\epsilon)$ smoothly varies from the I phase (with two energy gaps associated with three quasiparticle bands) to the C phase (with a single gap associated with two bands), even in the presence of a CDW. So as proven in Sec. III, the three bands of quasiparticles collapse into two bands in the C limit.

There is no doubt that higher harmonics such as the CDW play a crucial role in determining the IC phase boundary of Cr alloys. With no other harmonics present, the CDW destabilizes the I phase and shifts the IC phase boundary towards higher values of the energy mismatch z_0 .¹⁴ Kotani^{24,25} attempted to go beyond the three-band model by including both higher harmonics and neglected terms such as in Eq. (11). In Ref. 24, Kotani neglects harmonics higher than the CDW but includes an infinite hierarchy of terms like Eq. (11). In each such term, the Coulomb interaction $U(\mathbf{k}-\mathbf{k}'+\mathbf{Q}'_+-\mathbf{Q}'_-)$ is replaced by the same constant as the interaction $U(\mathbf{k}-\mathbf{k}')$. Unlike the three-band model, which allows a closed form solution, the infinite hierarchy of coupled equations generated by Kotani must be solved numerically. Kotani²⁵ later included the third harmonic of the SDW within this approach. Like the second harmonic, the third harmonic was also found to play an important role in determining the IC phase boundary.

Nonetheless, a rigorous solution of the RPA equations, including both the higher harmonics and the other terms neglected by the three-band model, has not yet been found. Instead of the procedure adopted by Kotani,²⁴ the Coulomb interaction $U(\mathbf{k}-\mathbf{k}'+\mathbf{Q}'_+-\mathbf{Q}'_-)$ should be separately expanded in cubic harmonics and replaced by a different lowest-order, constant term than $U(\mathbf{k}-\mathbf{k}')$. Such a rigorous solution of the RPA equations should eliminate the instability found within the three-band model as $\lambda'_3 \rightarrow \frac{1}{2}$.

In the most surprising result of our work, we find that the Coulomb interaction U' has important physical conse-

quences for both the I and C phases. In the I phase, the CDW amplitude grows with the size of U' . In the C phase, the ab and ba energies are shifted downwards by the Coulomb attraction U' between the excess holes on the b band and the electrons that transfer to the b band from the reservoir. When $\lambda'_2 > \lambda'_{2c}$, the energy shift is large enough to generate a first-order PC transition. Since the same Coulomb interaction is responsible for both the size of the ICDW and the first-order PC transition, we predict that the first-order PC transitions observed in CrFe and CrSi alloys are preceded by the growth of large CDW's in their I phases.

The growth of the CDW amplitude ϱ_0 with the Fe or Si concentrations should be straightforward to observe. As found in scattering measurements¹¹ and verified by the three-band model,^{2,14} the ratio ϱ_0/S_0^2 is relatively independent of temperature. But the three-band model also indicates¹⁴ that ϱ_0/S_0^2 is proportional to $1/(1-2\lambda'_3) = 1+4\lambda'_2$. So as the coupling parameter $\lambda'_2(x)$ increases with the Fe or Si concentration x , the ratio ϱ_0/S_0^2 should also increase. However, our phenomenological model does not tell us why Fe or Si doping should enhance the Coulomb attraction U' between electrons and holes on the b Fermi surface. Perhaps, first-principles calculations shall someday answer this question.

To summarize, we have provided a theoretical justification for the three-band model applied to the coupled spin and charge-density waves of I Cr alloys. Provided that the Coulomb constant λ' is suitably redefined, the three-band model reduces to the correct form in the C limit. We have also verified that the same Coulomb interaction U' that governs the size of the CDW in the I phase is also responsible for a first-order transition from the P to the C phase. Hopefully, future measurements of the ICDW in CrFe and CrSi alloys will confirm this prediction.

ACKNOWLEDGMENTS

One of us (R.F.) would like to acknowledge support from the U.S. Department of Energy under Contract No. DE-AC0586OR22464 with Lockheed Martin Energy Research Corp.

APPENDIX A: GREEN'S FUNCTIONS IN THE I PHASE

In imaginary time, the equations of motion for the Green's functions are summarized below, assuming that repeated spin indices are summed:

$$\begin{aligned} [-\partial/\partial\tau - \epsilon_a(\mathbf{k})]G(\mathbf{k}, \tau)_{\alpha\beta,aa} - \Delta_{\alpha\gamma}^{(+)}(\mathbf{k})G(\mathbf{k}, \tau)_{\gamma\beta,b+a} \\ - \Delta_{\alpha\gamma}^{(-)}(\mathbf{k})G(\mathbf{k}, \tau)_{\gamma\beta,b-a} = \delta_{\alpha\beta}\delta(\tau), \end{aligned} \quad (A1a)$$

$$\begin{aligned} [-\partial/\partial\tau - \epsilon_a(\mathbf{k})]G(\mathbf{k}, \tau)_{\alpha\beta,ab\pm} - \Delta_{\alpha\gamma}^{(+)}(\mathbf{k})G(\mathbf{k}, \tau)_{\gamma\beta,b+b\pm} \\ - \Delta_{\alpha\gamma}^{(-)}(\mathbf{k})G(\mathbf{k}, \tau)_{\gamma\beta,b-b\pm} = 0 \end{aligned} \quad (A1b)$$

$$\begin{aligned} [-\partial/\partial\tau - \epsilon_{b\pm}(\mathbf{k})]G(\mathbf{k}, \tau)_{\alpha\beta,b\pm b\pm} - \bar{\Delta}_{\alpha\gamma}^{(\pm)}(\mathbf{k})G(\mathbf{k}, \tau)_{\gamma\beta,ab\pm} \\ - \Gamma_{\alpha\gamma}^{(\pm\mp)}(\mathbf{k})G(\mathbf{k}, \tau)_{\gamma\beta,b\mp b\pm} = \delta_{\alpha\beta}\delta(\tau), \end{aligned} \quad (A1c)$$

$$[-\partial/\partial\tau - \epsilon_{b\pm}(\mathbf{k})]G(\mathbf{k}, \tau)_{\alpha\beta, b\pm a} - \bar{\Delta}_{\alpha\gamma}^{(\pm)}(\mathbf{k})G(\mathbf{k}, \tau)_{\gamma\beta, aa} \\ - \Gamma_{\alpha\gamma}^{(\pm\mp)}(\mathbf{k})G(\mathbf{k}, \tau)_{\gamma\beta, b\mp a} = 0 \quad (\text{A1d})$$

$$[-\partial/\partial\tau - \epsilon_{b\pm}(\mathbf{k})]G(\mathbf{k}, \tau)_{\alpha\beta, b\pm b\mp} - \bar{\Delta}_{\alpha\gamma}^{(\pm)}(\mathbf{k})G(\mathbf{k}, \tau)_{\gamma\beta, ab\mp} \\ - \Gamma_{\alpha\gamma}^{(\pm\mp)}(\mathbf{k})G(\mathbf{k}, \tau)_{\gamma\beta, b\mp b\mp} = \delta_{\alpha\beta}\delta_{Q'_+, Q'_-}. \quad (\text{A1e})$$

The equations of motion for the 6×6 matrix $\underline{G}(\mathbf{k}, \tau)$ can be easily converted to frequency space using

$$\underline{G}(\mathbf{k}, i\nu_l) = \int_0^\beta \underline{G}(\mathbf{k}, \tau) e^{i\nu_l\tau}, \quad (\text{A2})$$

where $\nu_l = (2l+1)\pi T$. We now impose¹⁸ the spin symmetries $G_{\alpha\beta, aa} = \delta_{\alpha\beta}G_{aa}$, $G_{\alpha\beta, ab\pm} = \hat{\mathbf{m}} \cdot \sigma_{\alpha\beta}G_{ab\pm}$, $G_{\alpha\beta, b\pm a} = \hat{\mathbf{m}} \cdot \sigma_{\alpha\beta}G_{b\pm a}$, $G_{\alpha\beta, b\pm b\pm} = \delta_{\alpha\beta}G_{b\pm b\pm}$, and $G_{\alpha\beta, b\pm b\mp} = \delta_{\alpha\beta}G_{b\pm b\mp}$. These relations imply that $\Delta_{\alpha\beta}^{(\pm)} = \hat{\mathbf{m}} \cdot \sigma_{\alpha\beta}\Delta^{(\pm)}$, $\bar{\Delta}_{\alpha\beta}^{(\pm)} = \hat{\mathbf{m}} \cdot \sigma_{\alpha\beta}\bar{\Delta}^{(\pm)}$, and $\Gamma_{\alpha\beta}^{(\pm\mp)} = \Gamma^{(\pm\mp)}\delta_{\alpha\beta}$. Consequently, we obtain the band matrix elements

$$G(\mathbf{k}, i\nu_l)_{b\pm a} = \frac{1}{D_3(\mathbf{k}, i\nu_l)} \{ \bar{\Delta}^{(\pm)}(\mathbf{k})(i\nu_l - \epsilon_{b\mp}(\mathbf{k})) \\ + \bar{\Delta}^{(\mp)}(\mathbf{k})\Gamma^{(\pm\mp)}(\mathbf{k}) \}, \quad (\text{A3a})$$

$$G(\mathbf{k}, i\nu_l)_{aa} = \frac{1}{D_3(\mathbf{k}, i\nu_l)} \{ [i\nu_l - \epsilon_{b+}(\mathbf{k})][i\nu_l - \epsilon_{b-}(\mathbf{k})] \\ - \Gamma^{(\pm\mp)}(\mathbf{k})D^{(\mp\pm)}(\mathbf{k}) \}, \quad (\text{A3b})$$

$$G(\mathbf{k}, i\nu_l)_{ab\pm} = \frac{1}{D_3(\mathbf{k}, i\nu_l)} \{ \Delta^{(\pm)}(\mathbf{k})[i\nu_l - \epsilon_{b\mp}(\mathbf{k})] \\ + \Delta^{(\mp)}(\mathbf{k})\Gamma^{(\mp\pm)}(\mathbf{k}) \}, \quad (\text{A3c})$$

$$G(\mathbf{k}, i\nu_l)_{b\mp b\pm} = \frac{1}{D_3(\mathbf{k}, i\nu_l)} \{ \Gamma^{(\mp\pm)}(\mathbf{k})[i\nu_l - \epsilon_a(\mathbf{k})] \\ + \Delta^{(\pm)}(\mathbf{k})\bar{\Delta}^{(\mp)}(\mathbf{k}) \}, \quad (\text{A3d})$$

$$G(\mathbf{k}, i\nu_l)_{b\pm b\pm} = \frac{1}{D_3(\mathbf{k}, i\nu_l)} \{ [i\nu_l - \epsilon_a(\mathbf{k})][i\nu_l - \epsilon_{b\mp}(\mathbf{k})] \\ - \Delta^{(\mp)}(\mathbf{k})\bar{\Delta}^{(\mp)}(\mathbf{k}) \}, \quad (\text{A3e})$$

where the denominator is

$$D_3(\mathbf{k}, i\nu_l) = [i\nu_l - \epsilon_a(\mathbf{k})][i\nu_l - \epsilon_{b+}(\mathbf{k})][i\nu_l - \epsilon_{b-}(\mathbf{k})] \\ - \Delta^{(+)}(\mathbf{k})\bar{\Delta}^{(+)}(\mathbf{k})[i\nu_l - \epsilon_{b-}(\mathbf{k})] \\ - \Delta^{(-)}(\mathbf{k})\bar{\Delta}^{(-)}(\mathbf{k})[i\nu_l - \epsilon_{b+}(\mathbf{k})] \\ - \Gamma^{(+)}(\mathbf{k})\Gamma^{(-)}(\mathbf{k})[i\nu_l - \epsilon_a(\mathbf{k})] \\ - \bar{\Delta}^{(-)}(\mathbf{k})\Delta^{(+)}(\mathbf{k})\Gamma^{(+)}(\mathbf{k}) \\ - \bar{\Delta}^{(+)}(\mathbf{k})\Delta^{(-)}(\mathbf{k})\Gamma^{(-)}(\mathbf{k}). \quad (\text{A4})$$

APPENDIX B: GREEN'S FUNCTIONS IN THE C PHASE

The Green's functions in the C phase obey the same symmetry relations as in Appendix A. We can easily obtain the equations of motion for the Green's functions so long as double counting is avoided. For example, terms with $\mathbf{q}=\mathbf{k}-\mathbf{k}'$ and $\mathbf{q}=\mathbf{k}-\mathbf{k}'+\mathbf{Q}'_+-\mathbf{Q}'_-$ are only counted once. We then find

$$[i\nu_l - \epsilon_a(\mathbf{k})]G(\mathbf{k}, i\nu_l)_{aa} - \Delta(\mathbf{k})G(\mathbf{k}, i\nu_l)_{ba} = 1, \quad (\text{B1a})$$

$$[i\nu_l - \epsilon_a(\mathbf{k})]G(\mathbf{k}, i\nu_l)_{ab} - \Delta(\mathbf{k})G(\mathbf{k}, i\nu_l)_{bb} = 0, \quad (\text{B1b})$$

$$[i\nu_l - \epsilon_{b+}(\mathbf{k})]G(\mathbf{k}, i\nu_l)_{bb} - \bar{\Delta}(\mathbf{k})G(\mathbf{k}, i\nu_l)_{ab} \\ - \Gamma(\mathbf{k})G(\mathbf{k}, i\nu_l)_{bb} = 1, \quad (\text{B1c})$$

$$[i\nu_l - \epsilon_{b+}(\mathbf{k})]G(\mathbf{k}, i\nu_l)_{ba} - \bar{\Delta}(\mathbf{k})G(\mathbf{k}, i\nu_l)_{aa} \\ - \Gamma(\mathbf{k})G(\mathbf{k}, i\nu_l)_{ba} = 0, \quad (\text{B1d})$$

where $G_{ab+} = G_{ab-} \equiv G_{ab}$, $G_{b+a} = G_{b-a} \equiv G_{ba}$, and $G_{b+b+} = G_{b-b-} = G_{b\pm b\mp} \equiv G_{bb}$. So only four independent matrix elements remain in the C phase.

The self-energies now obey the self-consistent relations

$$\Delta(\mathbf{k}) = -\frac{1}{V}T \sum_{l, \mathbf{k}'} U(\mathbf{k}-\mathbf{k}')G(\mathbf{k}', i\nu_l)_{ab}, \quad (\text{B2a})$$

$$\bar{\Delta}(\mathbf{k}) = -\frac{1}{V}T \sum_{l, \mathbf{k}'} U(\mathbf{k}-\mathbf{k}')G(\mathbf{k}', i\nu_l)_{ba}, \quad (\text{B2b})$$

$$\Gamma(\mathbf{k}) = -\frac{1}{V}T \sum_{l, \mathbf{k}'} U'(\mathbf{k}-\mathbf{k}')G(\mathbf{k}', i\nu_l)_{bb}. \quad (\text{B3})$$

APPENDIX C: LANDAU-GINZBURG EXPANSION

This appendix provides the coefficients in the Landau-Ginzburg expansion of the free energy $\Delta F_2(g, d)$ near the Néel temperature T_N . Starting with the free energy of Eq. (21), we expand

$$\sum_{l, \mathbf{k}} \ln \left| \frac{D_2(g, d, \mathbf{k}, i\nu_l)}{D_2(0, 0, \mathbf{k}, i\nu_l)} \right| \\ = \sum_{l, \mathbf{k}} \ln \left\{ 1 - \frac{2g^2 + d[i\nu_l - \epsilon_a(\mathbf{k})]}{[i\nu_l - \epsilon_a(\mathbf{k})][i\nu_l - \epsilon_{b+}(\mathbf{k})]} \right\} \quad (\text{C1})$$

in powers of g and d up to orders g^4 or d^2 . The coefficients in Eq. (28) are given by

$$A = \ln \left(\frac{T}{T_N^*} \right) - \sum_{n=0}^{\infty} \text{Re} \left(\frac{1}{X_n} - \frac{1}{n+1/2} \right), \quad (\text{C2a})$$

$$B = -\frac{1}{8\pi^2} \left(\frac{T_N^*}{T} \right)^2 \sum_{n=0}^{\infty} \text{Re} \left(\frac{1}{X_n^3} \right), \quad (\text{C2b})$$

$$C=0, \quad (\text{C2c})$$

$$D = \frac{1}{8\lambda'}, \quad (\text{C2d})$$

$$E = -\frac{1}{4\pi} \frac{T_N^*}{T} \sum_{n=0}^{\infty} \text{Im} \left(\frac{1}{X_n^2} \right), \quad (\text{C2e})$$

where X_n is defined by Eq. (35) in the text.

*Present address: Schindler Elevator Corporation, P. O. Box 1935, Morristown, NJ 07962-1935.

¹The properties of Cr alloys are reviewed by E. Fawcett, *Rev. Mod. Phys.* **60**, 209 (1988); E. Fawcett, H. L. Alberts, V. Yu. Galkin, D. R. Noakes, and J. V. Yakhmi, *ibid.* **66**, 26 (1994).

²C. Y. Young and J. B. Sokoloff, *J. Phys. F* **4**, 1304 (1974).

³K. Nakanishi and T. Kasuya, *J. Phys. Soc. Jpn.* **42**, 833 (1977).

⁴A. W. Overhauser, *Phys. Rev. Lett.* **4**, 226 (1960); *Phys. Rev.* **128**, 1437 (1962).

⁵W. M. Lomer, *Proc. Phys. Soc. London* **80**, 489 (1962).

⁶P. A. Fedders and P. C. Martin, *Phys. Rev.* **143**, 8245 (1966).

⁷S. Asano and J. Yamashita, *J. Phys. Soc. Jpn.* **23**, 714 (1967).

⁸R. S. Fishman and S. H. Liu, *Phys. Rev. B* **48**, 3820 (1993).

⁹Y. Tsunoda, M. Mori, N. Kunitomi, Y. Teraoka, and J. Kanamori, *Solid State Commun.* **14**, 287 (1974).

¹⁰A. F. Prekul and S. V. Sudareva, *Phys. Met. Metallogr.* **46**, 46 (1979).

¹¹R. Pynn, W. Press, S. M. Shapiro, and S. A. Werner, *Phys. Rev. B* **13**, 295 (1976).

¹²S. Iida, M. Khono, Y. Tsunoda, and N. Kunitomi, *J. Phys. Soc. Jpn.* **50**, 2581 (1981).

¹³J. P. Hill, G. Helgesen, and D. Gibbs, *Phys. Rev. B* **51**, 10 336 (1995).

¹⁴X. W. Jiang and R. S. Fishman, *J. Phys.: Condens. Matter* **9**, 3417 (1997); R. S. Fishman and X. W. Jiang, *J. Appl. Phys.* **81**, 4201 (1997).

¹⁵M. Mori and Y. Tsunoda, *J. Phys. C* **5**, L77 (1993).

¹⁶M. A. Lind and J. L. Stanford, *J. Phys. Soc. Jpn.* **53**, 4029 (1984).

¹⁷E. W. Fenton and C. R. Leavens, *J. Phys. F* **10**, 1853 (1980).

¹⁸The spin degrees of freedom of the Green's functions arise naturally if we start with the Hamiltonian

$$H = \sum_{\mathbf{k}, \sigma} \{ \epsilon_a(\mathbf{k}) a_{\mathbf{k}\sigma}^\dagger a_{\mathbf{k}\sigma} + \epsilon_b(\mathbf{k}) b_{\mathbf{k}\sigma}^\dagger b_{\mathbf{k}\sigma} \} \\ + \frac{1}{V} \sum_{\mathbf{q}, \mathbf{k}, \mathbf{k}', \alpha, \beta, \gamma, \delta} U_{\alpha\beta\delta\gamma}(\mathbf{q}) a_{\mathbf{k}\alpha}^\dagger b_{\mathbf{k}'\delta}^\dagger b_{\mathbf{k}'+\mathbf{q}\beta} a_{\mathbf{k}-\mathbf{q}\gamma} \\ + \frac{1}{2V} \sum_{\mathbf{q}, \mathbf{k}, \mathbf{k}', \alpha, \beta, \gamma, \delta} U'_{\alpha\beta\delta\gamma}(\mathbf{q}) b_{\mathbf{k}\alpha}^\dagger b_{\mathbf{k}'\delta}^\dagger b_{\mathbf{k}'+\mathbf{q}\beta} b_{\mathbf{k}-\mathbf{q}\gamma},$$

where

$$U_{\alpha\beta\delta\gamma}(\mathbf{q}) = \frac{1}{2} U(\mathbf{q}) (\hat{\mathbf{m}} \cdot \sigma_{\alpha\beta} \hat{\mathbf{m}} \cdot \sigma_{\delta\gamma} + \hat{\mathbf{e}} \cdot \sigma_{\alpha\beta} \hat{\mathbf{e}} \cdot \sigma_{\delta\gamma}),$$

$$U'_{\alpha\beta\delta\gamma}(\mathbf{q}) = \frac{1}{2} U'(\mathbf{q}) \delta_{\alpha\beta} \delta_{\delta\gamma}.$$

The unit vector $\hat{\mathbf{e}}$ is defined so that $\hat{\mathbf{e}} \cdot \hat{\mathbf{m}} = 0$ and the $\hat{\mathbf{e}}$ terms guarantee that U couples \uparrow and \downarrow spins in Eq. (5). It follows that $G(\mathbf{k}, i\nu_l)_{\alpha\beta, ab\pm} \propto \hat{\mathbf{m}} \cdot \sigma_{\alpha\beta}$ and $G(\mathbf{k}, i\nu_l)_{\alpha\beta, b\pm b\mp} \propto \delta_{\alpha\beta}$. The equations of motion in Appendix A are unchanged.

¹⁹H. Sato and K. Maki, *Int. J. Magn.* **4**, 163 (1973); **6**, 183 (1974).

²⁰N. Cowlam, G. E. Bacon, and L. Gillot, *J. Phys. F* **7**, L315 (1977).

²¹A. Shibatani, K. Motizuki, and T. Nagmiya, *Phys. Rev.* **177**, 984 (1969).

²²R. S. Fishman (unpublished).

²³R. S. Fishman and V. S. Viswanath, *Phys. Rev. B* **55**, 8347 (1997).

²⁴A. Kotani, *J. Phys. Soc. Jpn.* **38**, 974 (1975).

²⁵A. Kotani, *J. Phys. Soc. Jpn.* **41**, 1473 (1976).